Lattice dynamics of Ti-based pnictide superconductors $Ba_{1-x}Na_{x}Ti_{2}Sb_{2}O$

A. P. Litvinchuk, Phoung Doan, Zhongjia Tang, and Arnold M. Guloy

Phys. Rev. B **87**, 064505 — Published 15 February 2013

DOI: 10.1103/PhysRevB.87.064505

Lattice dynamics of Ti-based pnictide superconductors $Ba_{1-x}Na_xTi_2Sb_2O$

A. P. Litvinchuk
Texas Center for Superconductivity and Department of Physics, University of Houston, Houston, Texas 77204-5002, USA

Phoung Doan, Zhongjia Tang, and Arnold M. Guloy
Texas Center for Superconductivity and Department of Chemistry, University of Houston, Houston, Texas 77204-5003, USA
(Dated: February 4, 2013)

The lattice dynamics of layered $Ba_{1-x}Na_xTi_2Sb_2O$ pnictides ($0 \leq x \leq 0.3$) is studied experimentally by means of Raman scattering and theoretically within the density functional theory. Both symmetry allowed Raman-active modes are observed in the spectra and assigned to the lattice eigenmodes: z-axis motion of Sb ions (A_{1g}-symmetry mode) and in-xy-plane displacement of Sb (E_g-symmetry vibration). Calculated and experimental frequencies of these modes are found to be in good agreement. The E_g mode exhibits a non-monotonous dependence of its frequency upon doping, which is found to correlate with the variation of Sb-Ti distances and strength of the interaction between Ti_2Sb_2O slabs.

PACS numbers: 74.70.Xa; 74.20.Pq; 74.25.nd; 63.20.D-

The discovery of Fe-based pnictide superconductors ($LaFeAsO_{1-x}F_x$) several years ago[1–3] has followed by an intense wave of developments in a search of novel materials with superconducting properties. Over the years several related classes of superconducting materials were identified, such as doped $A_{1-x}(Sr/Ba)_xFe_2As_2$[4,5] and intrinsic LiFeAs[6], for example. Even though the highest critical superconducting temperature T_c of these materials does not exceed 55K, considerable progress has been made over the years in understanding their properties. The unconventional nature of the superconductivity was clearly established both theoretically and experimentally with magnetic excitations (spin density density waves) being at the heart of the pairing mechanism[7,8]. Thus, a strong competition between magnetism and superconductivity has been established (see, e.g. Ref. 9,10 and references therein). As far as optical spectroscopy results, phonon and electronic Raman scattering and infrared reflection experiments on various classes of iron pnictides were detrimental in monitoring specific lattice dynamical features due to non-vanishing electron-phonon interaction[11–14] and structural phase transitions,[15,16] establishing the gap symmetry and a multi-gap behavior,[17,18] as well as a pseudogap regime.[19]

Recently, a new class of transition-element pnictide oxide was shown to exhibit superconducting properties upon proper doping: $BaTi_2Sb_2O$[20]. The Na^+ for Ba^{2+} substitution leads to a suppression of the spin density waves phase and material exhibits bulk superconductivity within the doping range $0.05 < x < 0.33$, with the critical temperature reaching its maximum T_c=5.5 K at $x \approx 0.15$.

We will further focus on the dynamical properties of the lattice of $Ba_{1-x}Na_xTi_2Sb_2O$. The group theoretical analysis of lattice vibrations is performed and the activity of vibrational mode is determined. Further, performed density functional calculations yield mode frequencies and the displacement pattern for all optical modes. These results are compared with the experimental Raman scattering data.

Single crystals of $BaTi_2Sb_2O$ were synthesized by high-temperature reactions of the appropriate starting materials in welded Nb containers, as described earlier in Ref. 20. The crystallographic structure of $BaTi_2Sb_2O$, shown in Fig. 1, features the antiperoskite-type Ti_2O layers (similar, but "inverse" to the CuO_2 layers in cuprates), that are capped by Sb atoms on both sides.

All Raman scattering spectra were measured in the backscattering geometry at room temperature on a Horiba Jobin Yvon T-64000 triple spectrometer equipped with an optical microscope and a liquid nitrogen cooled CCD detector. The spectral resolution did not exceed 1.0 cm^{-1}. An Ar^+ laser ($\lambda_{las} = 514.5$ nm) for used for the excitation excitation. The incident laser power was kept below 1.0 mW in order to minimize heating of the sample.

The results of the group theoretical analysis of lattice vibrations of $BaTi_2Sb_2O$ (space group $P4/mmm$) are summarized in Table I. Ba, Ti, and O ions occupy centrosymmetric lattice sites and consequently none of them contributes to the even-parity Raman active vibrations. Thus, only two Sb-related modes are expected to be observed in Raman spectra: A_{1g} due to the z-axis displacement, and the doubly degenerate E_g due to motion within the xy-plane.

The first principle calculations of the electronic ground state of Na-doped $BaTi_2Sb_2O$ were performed within the generalized-gradient approximation with Perdew-Burke-Ernzerhof[22] local functional, using the CASTEP code.[23] The norm-conserving pseudopotentials and experimental lattice parameters of the crystal[20] were used. For self-consistent calculations of the electronic structure and other relevant electronic properties the integration over the Brillouin zone was performed over the $25 \times 25 \times 13$ Monkhorst-Pack grid[24] in the reciprocal space. These results are found to be in

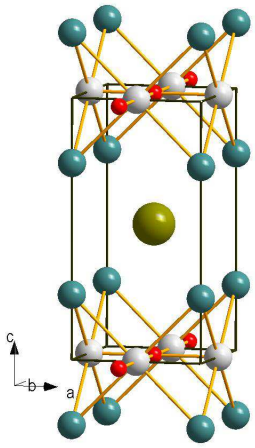

FIG. 1: (Color on line) The crystallographic structure of $BaTi_2Sb_2O$, featuring Sb_2Ti_2O slabs (blue, grey and small red spheres, respectively). Ba atoms are shown in green.

TABLE I: Wyckoff position, cite symmetry and irreducible representations of the nonequivalent atomic sites in the $P4/mmm$ structure of $BaTi_2Sb_2O$.[20,21]

Atom	Wyckoff notation	Cite symmetry	Irreducible representantions
Ba	1d	$4/mmm$	$A_{2u} + E_u$
Ti	2f	mmm	$A_{2u} + B_{2u} + 2E_u$
Sb	2g	$4mm$	$A_{1g} + A_{2u} + E_g + E_u$
O	1c	$4/mmm$	$A_{2u} + E_u$

Modes classification
$\Gamma_{\text{acoustic}} = A_{2u} + E_u$
$\Gamma_{\text{Raman}} = A_{1g} + E_g$
$\Gamma_{\text{IR}} = 3A_{2u} + 4E_u$

good agreement with those reported recently by Singh[25]. In particular, the Fermi surface clearly shows the existence of nearly parallel sheets, a fact which points towards magnetic instability of the parent compound[26,27].

The lattice dynamics of $BaTi_2Sb_2O$ was calculated within the local density approximation with Perdew-Wang local functional[28], using DMol^3 code[29,30] by means of finite displacements method. The frequencies of all optical Brillouin zone center modes are listed in Table II. Two of them, the even-parity A_{1g} and E_g, are Raman-active, seven odd-parity vibrations (A_{2u} and E_u) are infrared-active, and there is also one silent mode (B_{2u}).

In Fig. 2 Raman spectra of $Ba_{1-x}Na_xTi_2Sb_2O$ crystals are shown for several compositions x. In the parent compound two lines are clearly distinguished in the spectra which, according the DFT calculations, correspond to the in-xy-plane E_g (126 cm^{-1}) and z-axis A_{1g} (152 cm^{-1}) modes; their displacement pattern is shown in the lower part of Fig. 3. This latter mode shift slightly and monotonously towards smaller wavenumbers upon doping in the whole concentration range. The lower frequency E_g vibration exhibits much larger shifts and, more importantly, a non-linear behavior: upon doping its frequency first increases, reaches the maximum around $x \approx 0.15$, and further

TABLE II: Calculated and experimental frequencies (in cm^{-1}) of optical vibrations $BaTi_2Sb_2O$ and their assignment. A_{2u} and E_u modes are infrared active.

Mode	Frequency calculated	Frequency experimental	Assignment
A_{1g}	158	152	Sb - z-axis
E_g	110	126	Sb - xy plane
$A_{2u}(1)$	82		Ba - z-axis
$A_{2u}(2)$	226		O+Ti - z-axis
$A_{2u}(3)$	290		O − Ti - z-axis
$E_u(1)$	72		Ba−(Ti+O) - xy plane
$E_u(2)$	146		(Ti+O)−Sb - xy plane
$E_u(3)$	263		Ti - xy plane
$E_u(4)$	446		O - xy plane
B_{2u}	221	silent	Ti- z axis

decreases, as shown in the upper part of Fig. 3.

In Fig. 4 the variation of the lattice parameters of the crystallographic unit cell of $Ba_{1-x}Na_xTi_2Sb_2O$ is presented, which shows monotonous compression upon doping of the unit cell within the xy-plane due to smaller Na^+ ionic radius in comparison to Ba^{2+}. The c-axis lattice parameter exhibits, however, a non-monotonous behavior: the unit cell initially slightly contracts upon doping, and further (for $x \geq 0.15$) starts to expand. The DFT calculation results, presented in the two lowest panels of Fig. 4, show that this behavior is also valid for the inter-atomic $(Sb\text{-}Sb)_z$ distance along c-axis within the Sb_2Ti_2O slab.

In relation to the doping dependence of the vibrational modes, the A_{1g} involves both stretching and bending of Sb-Ti bonds and for a fixed cation-anion interaction strength its frequency is expected to increase as a results of a shortening of corresponding bonds. Experimentally, however, the A_{1g} mode frequency decreases slightly upon doping, which signals some weakening of the Sb-Ti interaction due to charge redistribution. More interesting is that the "slab thickness", which is characterized by the Sb-Sb distance along the c-axis, shows a non-monotonous change upon doping: it initially shrinks, but starts to expand for $x > 0.15$. And this is directly reflected in a pronounced softening of the E_g mode in the same concentration range $x > 0.15$. It is important to note that the superconducting critical temperature T_c also reaches its maximum around $x \approx 0.15$ (Ref. 20), and its drop upon further doping could be related to a weakening of Sb-Ti and inter-slab interactions.

In summary, Raman scattering spectra of superconducting layered $Ba_{1-x}Na_xTi_2Sb_2O$ single crystals have been measured and both allowed by symmetry modes were observed experimentally and assigned to the z-axis (A_{1g} symmetry) and xy-plane (E_g symmetry) vibrations of Sb ions. Their frequencies are in good agreements with those calculated within the density functional theory. A non-monotonous dependence of the position of the E_g mode is found upon doping, which is shown to correlate with the Sb-Ti spacing and interaction between Sb_2Ti_2O slabs.

This work was supported in part by the the State of Texas through TcSUH. A.M.G. acknowledge the support from

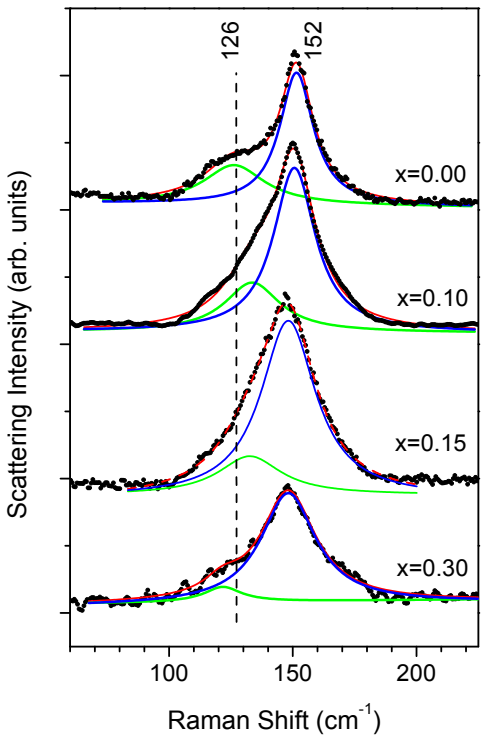

FIG. 2: (Color on line) Raman scattering spectra of $Ba_{1-x}Na_xTi_2Sb_2O$ as obtained at room temperature with $\lambda_{exc} = 514.5$ nm excitation (solid point) and their decomposition into two Lorentzian lines. Spectra are shifted vertically for clarity. The vertical dotted line marks the position of the low-energy phonon mode for the parent compound $x = 0$. Note a non-monotonous shift of this mode upon doping.

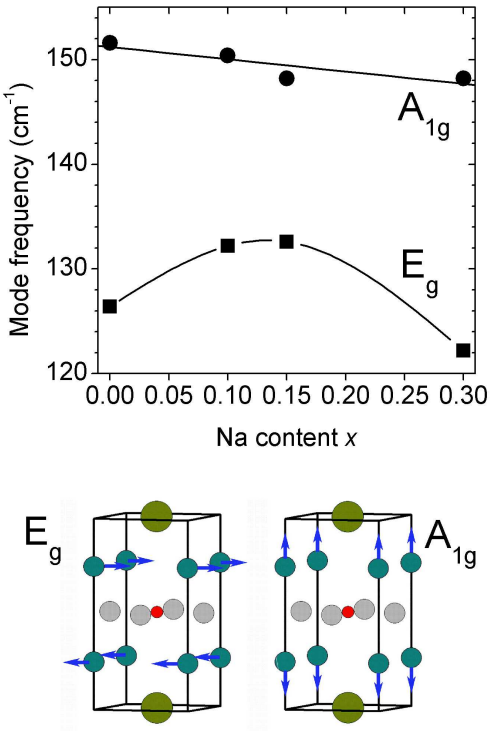

FIG. 3: (Color on line) The position of modes in the Raman scattering spectra of $Ba_{1-x}Na_xTi_2Sb_2O$ as a function of doping x (lines are a guide to the eye). Calculated displacement patterns for both modes are shown in the lower part of the Figure (lower frequency E_g mode on the left and higher frequency A_{1g} mode on the right).

the NSF (CHE-0616805) and the R.A. Welch Foundation.

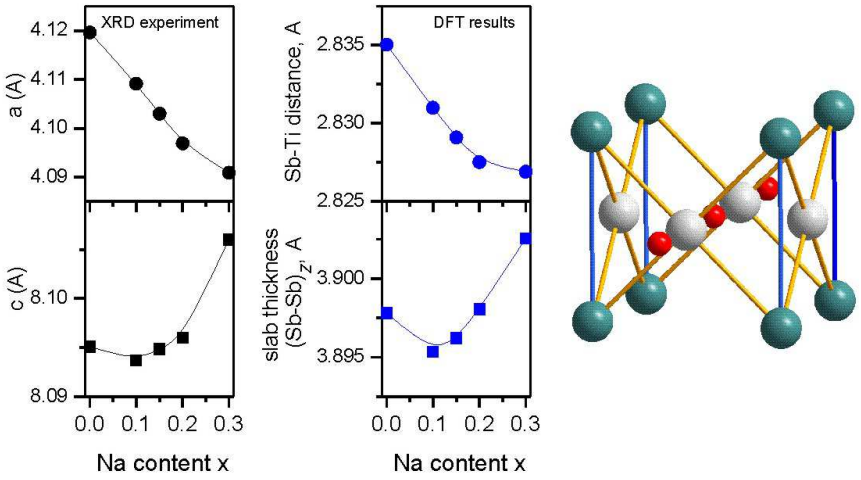

FIG. 4: (Color on line) Experimental crystal lattice parameters a and c (X-ray diffraction data) of $Ba_{1-x}Na_xTi_2Sb_2O$ as a function of doping are shown in on the left panel. The DFT-calculated Sb_2Ti_2O "slab thickness" $(Sb\text{-}Sb)_z$ (blue vertical lines in the picture on the right) and the Sb-Ti distance of a relaxed unit cell (yellow lines) are presented in the middle panel. Lines are a guide to the eye. Note a non-monotonous behavior upon doping of the c-axis parameter and the "slab thickness" $(Sb\text{-}Sb)_z$.

[1] Y. Kamihara, T. Watanabe, M. Hirano, and H. Hosono, J. Am. Chem. Soc. **130**, 3296 (2008).
[2] H. Takahashi, K. Igawa, K. Arii, Y. Kamihara, M. Hirano, and H. Hosono, Nature **453**, 376 (2008).
[3] X.H. Chen, T. Wu, G. Wu, R.H. Liu, H. Chen, and D.F. Fang, Nature **453**, 761 (2008).
[4] M. Rotter, M. Tegel, and D. Johrendt, Phys. Rev. Lett. **101**, 107006 (2008).
[5] K. Sasmal, Bing Lv, B. Lorenz, A.M. Guloy, F. Chen, Y.-Y. Xue, and C.W. Chu, Phys. Rev. Lett. **101**, 107007 (2008).
[6] J.H. Tapp, Z. Tang, Bing Lv, K. Sasmal, B. Lorenz, P.C.W. Chu, and A.M. Guloy, Phys. Rev. B **78**, 060505R (2008).
[7] I.I. Mazin, D.J. Singh, M.D. Johannes, and M.H. Du, Phys. Rev. Lett. **101**, 057003 (2008).
[8] P.J. Hirschfeld, M.M. Korshunov, and I.I. Mazin, Rep. Progr. Phys. **74**, 124508 (2011).
[9] J. Zhao, D.T. Adroja, D.-X. Yao, R. Bewley, S. Li, X.F. Wang, G. Wu, X.H. Chen, J. Hu, and P. Dai, Nature Phys. **5**, 555 (2009).
[10] D.N. Basov and A.V. Chubukov, Nature Phys. **7**, 273 (2011).
[11] A.P. Litvinchuk, V.G. Hadjiev, M.N. Iliev, Bing Lv, A.M. Guloy, and C.W. Chu, Phys. Rev. B **78**, 060503R (2008).
[12] L. Chauviére, Y. Gallais, M. Cazayous, A. Sacuto, M.A. Méasson, D. Colson, and A. Forget, Phys. Rev. B **80**, 094504 (2009).
[13] K.-Y. Choi, P. Lemmens, I. Eremin, G. Zwicknagl, H Berger, G.L. Sun, D.L. Sun, and C.T. Lin, J. Phys. Cond. Matter **22**, 115802 (2010).
[14] A.P. Litvinchuk, Bing Lv, and C.W. Chu, Phys. Rev. B **84**, 092504 (2011).
[15] K.-Y. Choi, D. Wulferding, P. Lemmens, N. Ni, S.L. Bud'ko, and P.C. Canfield, Phys. Rev. B **78**, 212503 (2008).
[16] A. Ignatov, A. Kumar, P. Lubik, R.H. Yuan, W.T. Guo, N.L. Wang, K. Rabe, and G. Blumberg, Phys. Rev. B **86**, 134107 (2012).
[17] G.R. Boyd, T.P. Devereaux, P.J. Hirschfeld, V. Mishra, and D.J. Scalapino, Phys. Rev. B **79**, 174521 (2009).
[18] B. Muschler, W. Prestel, R. Hackl, T.P. Devereaux, J.G. Analytis, J.-H. Chu, and I.R. Fisher, Phys. Rev. B **80**, 180510R (2009).
[19] S.J. Moon, A.A. Schafgans, S. Kasahara, T. Shibauchi, T. Terashima, Y. Matsuda, M.A. Tanatar, R. Prozorov, A. Thaler, P.C. Canfield, A.S. Sefat, D. Mandrus, and D.N. Basov, Phys. Rev. Lett. **109**, 027006 (2012).
[20] P. Doan, M. Gooch, Z. Tang, B. Lorenz, A. Möller, J. Tapp, P.C.W. Chu, and A.M. Guloy, J. Am. Chem. Soc. **134**, 16520 (2012).
[21] D.L. Rousseau, R.P. Bauman, and S.P.S. Porto, J. Raman Spectr. **10**, 253 (1981).
[22] J.P. Perdew, K. Burke, and M. Ernzerhof, Phys. Rev. Lett. **77**, 3865 (1996).
[23] S.J. Clark, M.D. Segall, C.J. Pickard, P.J. Hasnip, W.J. Probert, K. Refson, and M.C. Payne, Z. Kristallogr. **220**, 567 (2005).
[24] H.J. Monkhorst and J.D. Pack, Phys. Rev. **13**, 5188 (1976).

[25] D.J. Singh, New J. Phys. **14**, 123003 (2012).
[26] E. Canadell and M.-H. Whangbo, Chem. Rev. **91**, 965 (1991).
[27] W.E. Picket, Phys. Rev. B **58**, 4335 (1998).
[28] J.P. Perdew and Y. Wang, Phys. Rev. B **45**, 13244 (1992).
[29] B.J. Delley, Phys. Chem. **100**, 6107 (1996).
[30] B.J. Delley, J. Chem. Phys. **113**, 7756 (2000).